

Nanoporous Transparent MOF Glasses with Accessible Internal Surface

Yingbo Zhao,[†] Seung-Yul Lee,[‡] Nigel Becknell,[†] Omar M. Yaghi,^{*,†,§} and C. Austen Angell^{*,‡}

[†]Department of Chemistry, University of California at Berkeley, and Materials Sciences Division, Lawrence Berkeley National Laboratory, Kavli Energy NanoSciences Institute at Berkeley, Berkeley, California 94720, United States

[‡]School of Molecular Sciences, Arizona State University, Tempe, Arizona 85287-1604, United States

[§]King Abdulaziz City for Science and Technology, Riyadh 11442, Saudi Arabia

S Supporting Information

ABSTRACT: While glassy materials can be made from virtually every class of liquid (metallic, molecular, covalent, and ionic), to date, formation of glasses in which structural units impart porosity on the nanoscopic level remains undeveloped. In view of the well-established porosity of metal–organic frameworks (MOFs) and the flexibility of their design, we have sought to combine their formation principles with the general versatility of glassy materials. Although the preparation of glassy MOFs can be achieved by amorphization of crystalline frameworks, transparent glassy MOFs exhibiting permanent porosity accessible to gases are yet to be reported. Here, we present a generalizable chemical strategy for making such MOF glasses by assembly from viscous solutions of metal node and organic strut and subsequent evaporation of a plasticizer–modulator solvent. This process yields glasses with 300 m²/g internal surface area (obtained from N₂ adsorption isotherms) and a 2 nm pore–pore separation. On a volumetric basis, this porosity (0.33 cm³/cm³) is 3 times that of the early MOFs (0.11 cm³/cm³ for MOF-2) and within range of the most porous MOFs known (0.60 cm³/cm³ for MOF-5). We believe the porosity originates from a 3D covalent network as evidenced by the disappearance of the glass transition signature as the solvent is removed and the highly cross-linked nanostructure builds up. Our work represents an important step forward in translating the versatility and porosity of MOFs to glassy materials.

Conceptually, metal–organic framework (MOF) glasses with permanent porosity can be constructed by applying reticular chemistry to conventional glasses (e.g., silicate glasses),¹ where the silicon atom is replaced by a metal cluster (metal node) and the bridging oxygen atom is replaced by a ditopic organic linker (organic strut) that linked to the metal node. According to constraint theory,² the stability of this expanded network should be equivalent to that of the conventional glass in terms of the balance between constraints and degrees of freedom. However, in this case, similar to the “isoreticular expansion” known in crystalline MOFs, the void volume of the system should become a strong function of the length of the strut, the size of the cluster node, and the manner of connection between them. Thus, we should be able to combine the maximum (strain-

free) rigidity condition with a large empty space condition, thereby producing nanoporous glasses. We now expect the range of nanoporous MOF glass compositions to greatly exceed those found in atomic systems such as the classical Ge–As–Se system for which the original “magic” stability condition, $\langle r \rangle = 2.4$ ($\langle r \rangle$, the average bond density), was deduced.^{2a}

Previously, reports of MOF glasses were based on destructive treatments (i.e., thermally induced amorphization) of crystalline MOFs.³ However, these treatments exclusively led to compromised porosity, and these MOF glasses were not accessible to gases (no surface area based on N₂ isotherm has been reported).⁴ Other reported amorphous MOFs, although sometimes having gas uptake, are essentially amorphous mass, the light scattering by which excludes any description as a “glass”.⁵ Glasses can be taken through a thermodynamic cycle that includes passage into the liquid state and return to the same state they started from provided the same thermal protocol is followed. Another class of solution-processable porous material, polymers with intrinsic porosity, has pure organic composition and consists of irregularly packed organic chains⁶ thus is fundamentally different from the 3D MOF frameworks developed in this report.

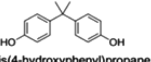
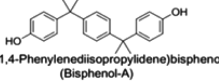
Herein, we use a constructive approach to obtain monolithic, transparent nanoporous MOF glasses, which relies on a solvent modulator that dissolves the organic linker and competitively coordinates to the metal nodes. This solvent modulator is analogous to monodentate modulators used to tune the morphology and crystallinity of MOFs (e.g., acetic acid in the synthesis of UiO-66).⁷ The synthetic procedure we developed starts by dissolving the metal nodes and organic linker in the solvent modulator to form a liquid. The gradual removal of the solvent modulator from the liquid by evaporation enables the linker to coordinate to the metal nodes and form MOF networks with increasing completeness (or connectivity). This process proceeds until the liquid turns into a glassy solid, which has the robustness and porosity of a MOF but the shape of a liquid.

The organic linkers we chose to demonstrate this chemistry are bisphenols (Table 1), and the corresponding modulator, *m*-cresol, is an extraordinary solvent for polymeric compounds (to keep the dynamically forming network dissolved) that is volatile enough for facile evaporation.⁸ The metal nodes we used are titanium-oxo (Ti-oxo) clusters,⁹ which form labile covalent

Received: July 8, 2016

Published: August 18, 2016

Table 1. Various Bisphenol Struts Used in Glassy MOF Synthesis

| strut character | Structure formula and chemical name (common name) | Abbreviation | T_m (°C) | T_g (°C) |
|-----------------|--|--------------|------------|------------|
| rigid |  1,4-benzenediol (Hydroquinone) | HQ | 171 | – |
| rigid |  2,2-Bis(4-hydroxyphenyl)propane (Bisphenol-A) | BPA | 158 | 35.8 |
| semi-rigid |  4,4'-(1,4-Phenylenediisopropylidene)bisphenol (Bisphenol-A) | BPP | 193 | 44.1 |

bonds with phenols that can support a 3D porous network and allow for the necessary dynamic ligand exchange.^{9b,10} The $Ti_{16}O_{16}(OEt)_{32}$ cluster (Figure 1a) is known to undergo facile ligand exchanges with phenol and alcohols without the decomposition of the $Ti_{16}O_{16}$ core.^{9b}

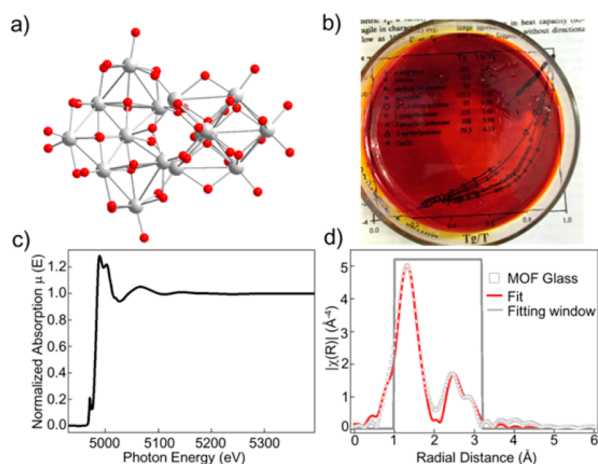


Figure 1. MOF glass is composed of Ti-oxo clusters linked with bisphenol linkers. (a) Structure core of $Ti_{16}O_{16}(OEt)_{32}$: Ti, gray; O, red; ethoxides are omitted for clarity. (b) Photograph of monolithic MOF glass in a 10 cm diameter Petri dish, following vitrification by *m*-cresol evaporation. (c) X-ray absorption spectrum of the MOF glass and (d) fitting of $Ti_{16}O_{16}(OEt)_{32}$ structure model to EXAFS of the MOF glass.

The Ti-oxo cluster was synthesized according to literature reports,^{9b} where titanium ethoxide was reacted with water in ethanol to give single crystals of $Ti_{16}O_{16}(OEt)_{32}$ (section S2). This cluster was then reacted with BPA linkers in THF at reflux overnight, where the ethoxide ligand was replaced by phenolates to form a network (section S2). This network can be dissolved in cresol with heating, and subsequent evaporation of cresol at 140 °C gives monolithic, transparent glasses. It was during this process that the Ti-cresolate-type bonds of the broken network were systematically replaced by bridging bonds of the Ti–O–(strut)–O–Ti type, as can be followed by monitoring the glass transition temperature (T_g) versus weight fraction of *m*-cresol (see below). This MOF glass can also be obtained by using titanium alkoxide as precursor, and the Ti-oxo clusters can be formed in situ during the reaction (section S2). The transparent orange monolithic glassy product of this process is shown in Figure 1b. This Ti-BPA MOF glass is insoluble in water and common organic solvents such as DMF, acetonitrile, THF, and acetone and only soluble in cresol when heated, indicating the

glass is an extended network instead of an irregular assembly of molecular oligomers.

Removal of solvent to vitrify an assembly of large molecules has actually long been used as a means of preparing glassy solids. The solvent removal plays a role analogous to that of cooling a liquid of fixed composition, by decreasing the configurational freedom of the large molecules in a solution. According to the celebrated Adam–Gibbs equation, viscosity rises exponentially with configurational entropy (S_c) decrease,¹¹ until the shear relaxation time reaches the order of minutes and the structure “freezes” for experiments of that time scale. In the MOF glasses case, configurational restrictions are accelerated by the formation of the covalent bridging node–node linkages. There are some similarities in our process to the formation of hydrocarbon-containing silicas (ormosils).¹² However, the organic components of ormosils were highly flexible hydrocarbon chain fragments and quite different in their function from that of the Table 1 struts. No generation of porosity was sought nor detected.

We confirmed the presence of Ti-oxo clusters as metal nodes in the MOF glasses by X-ray absorption spectroscopy at the Ti K-edge (section S3). The pre-edge feature is similar to that of neptunite and indicates Ti is six-coordinated,¹³ which is consistent with the chemical environment of Ti in the Ti-oxo cluster $Ti_{16}O_{16}(OEt)_{32}$ (Figure 1c). Also, the position, area, and line shape of the pre-edge peak contradicts known phases of TiO_2 .¹³ Extended X-ray absorption fine structure (EXAFS) also supported the presence of Ti-oxo clusters, as the $Ti_{16}O_{16}(OEt)_{32}$ model cluster can be successfully fit to the EXAFS data acquired for the MOF glass (Figure 1d and Tables S1 and S2). Specifically, the path length for the first Ti–Ti scattering was found to be around 3.04–3.07 Å, which resembles the path lengths of Ti–Ti scatterers in the Ti-oxo cluster, and the number of Ti–Ti scatterers found confirmed the absence of Ti–O–Ti dimers typically found in Ti-phenol networks.¹⁴ Analysis by X-ray absorption spectroscopy clearly showed that the MOF glass is composed of Ti-oxo clusters as the metal node, although it cannot rule out the presence of other Ti-oxo clusters with structures similar to $Ti_{16}O_{16}(OEt)_{32}$ [e.g., $Ti_{12}O_{16}(O-iPr)_{16}$].^{9a} This is consistent with the chemical composition analysis of the MOF glass, where elemental analysis, NMR (section S4, Figures S1 and S2) and ICP-AES were combined to give a typical chemical formula of $Ti_{16}O_{16}(BPA)_x(OR)_{32-x}$ ($x \sim 4$, OR is cresolate, hydroxide, and ethoxide; section S4). IR spectroscopy was used to confirm the incorporation and integrity of the BPA linkers in the glass (Figure S4). From X-ray absorption spectroscopy and chemical composition analysis, we confirmed that the Ti-BPA MOF glasses are composed of Ti-oxo clusters linked with BPA. Ti-BPP, a derivative of the Ti-BPA glass constructed with Ti-oxo clusters and BPP linkers, was synthesized and characterized in a similar manner (sections S2 and S4). These glasses were activated by being washed with acetone, methanol, or ethanol, exchanged with supercritical CO_2 , and heated under dynamic vacuum to remove residual bisphenols and unbonded cresol molecules (section S2). Activated MOF glasses were subjected to further characterization and remained transparent, free-standing, and monolithic (Figure S5).

The structures of the above-mentioned Ti-BPA glass and its derivative Ti-BPP glass were characterized by X-ray powder diffraction, which gave dominant low-angle peaks in the vicinity of $2\theta = 2-5^\circ$, corresponding to pore–pore separations of about 2 nm, comparable to those known for crystalline zeolite A (Figure 2a).¹⁵ Transmission electron microscopy (TEM) was

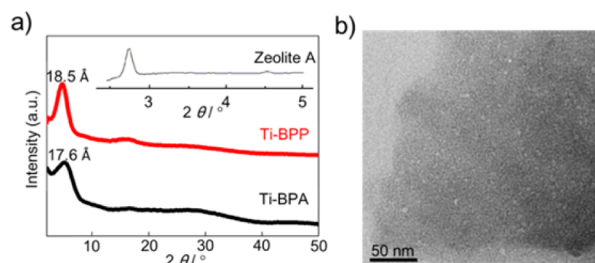


Figure 2. Structural characterization of the MOF glasses. (a) XRD pattern for MOF glasses with (i) BPP struts and (ii) BPA struts, compared with the low-angle line of zeolite A (internal pore dimension = 25 Å).¹⁵ Prominent low-angle peaks $2\theta =$ (i) 4.8° and (ii) 5.0° correspond to 18.5 and 17.6 Å d -spacings in a crystalline material. (b) Typical TEM image of the MOF glass (Ti-BPP) showing the absence of lattice fringes.

employed to confirm the absence of crystallinity, as no lattice fringes were observed for Ti-BPP and Ti-BPA glasses, with a typical image shown in Figure 2b.

The accessible internal surface of the MOF glasses is clearly demonstrated by N_2 adsorption isotherms. According to the adsorption isotherm shapes of Figure 3, the accessible internal

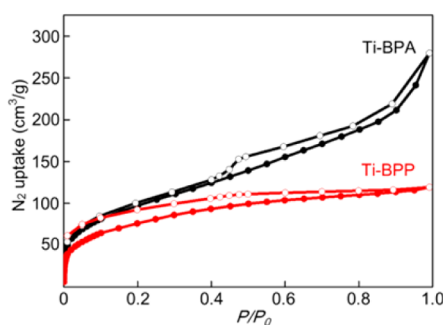


Figure 3. N_2 adsorption isotherms (77 K) for MOF glasses. Ti-BPA g-MOF shows highly reversible behavior at low gas uptake. From these data, we calculate internal surface values of 330 and 267 m^2/g . Due to the high backbone density measured by He pycnometry, i.e., 2.7 g/cm^3 for Ti-BPP, these MOFs are actually more porous than the surface area indicates. In the case of Ti-BPP, it has free volume of 0.33 cm^3/cm^3 , with volumetric N_2 uptake of 216 cm^3/cm^3 .

surface is heterogeneously distributed, which is not surprising for a glassy material. The total internal surface area, which is the important quantity, is 330 m^2/g for the Ti-BPA MOF glass and 267 m^2/g for the Ti-BPP MOF glass. The latter result was obtained for three separate preparations of this material. Its lower value than for the Ti-BPA shows that the naive picture of a strut-length-dependent internal surface is inaccurate, no doubt due to the nonrigid nature of the single oxygen link to the node combined with the extra sp^3 carbon in the strut. It is reasonable to expect that the dissolution–evaporation vitrification principle that we have introduced here will permit extensions to more rigid node–strut connections. Either of the above compares favorably with the most porous glass that has previously been made by physical methods (Corning “thirsty glass”, 250 m^2/g , made by laborious phase separation and leaching method).¹⁶ In the case of the BPA struts, the gas uptake is quite reversible. Hysteresis is only in evidence for the higher uptake levels and even then is not very pronounced.

The internal surface of our MOF glass can be better understood when the high density of the framework is taken

into account and a volumetric measure for porosity is used. The framework density can be obtained by the helium pycnometry method which, applied to our Ti-BPP g-MOF samples, yields a value of 2.7 g/cm^3 . From this, we derive a N_2 uptake volume of 216 cm^3/cm^3 of glass corresponding to 33% open space; a value that places g-MOF at higher porosity than the first porous MOF (MOF-2, 11%) and in the range of typical MOFs (MOF-5, 60%).^{1b}

We further consider an interesting aspect of the T_g signature by which the cohesive energy of a glassy phase is commonly assessed¹⁷ and by which the properties of the liquid phase above T_g are commonly scaled.¹⁸ The Ti-BPA and Ti-BPP glasses, with 3D network structure, prove to imitate very dry silica,¹⁹ vitreous water in its low-density polyamorphic (LDA) form,²⁰ and also most of the common ambers (highly cross-linked organic glasses from geologically distant times). These are all problematic because their T_g 's are undetectable except by very sensitive measurements. In the known cases, like the present one, they seem to become systematically nonexistent (the C_p jump, ΔC_p , disappears) as the modulator (or network breaking component) is removed. The significance of vanishing T_g to theory of the T_g is currently at the center of debate. For fragile liquids, configurational heat capacities [$C_{p(\text{conf})}$] usually increase as T_g is approached, whereas for the smaller number of very strong liquids, the opposite is true, with $C_{p(\text{conf})}$ disappearing in some cases. In the “super strong” cases of water and a-Si, “ubiquitous” glass signatures disappear,²¹ including excess entropy in the case of LDA water,²² meaning its glass is in a unique low entropy state (“perfect” glass).^{22,23} Disappearance of ΔC_p in our g-MOF is intriguing and will be the focus of future investigation.

Figure 4 shows the behavior of Ti-BPA solution in cresol (section S2), as the wt % of the Ti-BPA network was increased from effectively 0 (1.27 wt %) to the 50 wt % domain. As in polymer-plus-plasticizer phenomenology,²⁴ a highly nonlinear relationship between T_g and macromolecule content was found, but unlike the chain polymer case, the strength of T_g also diminishes. Beyond 50 wt % Ti-BPA, T_g cannot be detected by

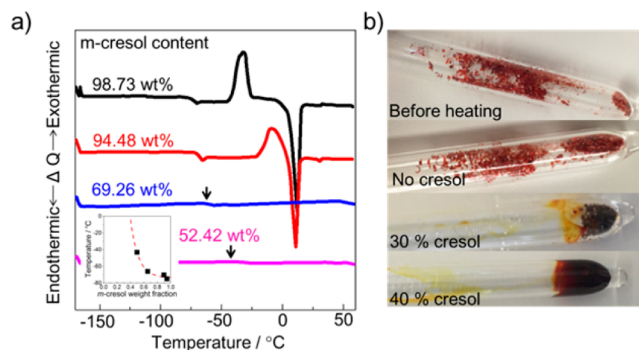


Figure 4. T_g of Ti-BPA solution. (a) Differential scanning calorimetry thermograms of Ti-BPA in m -cresol solutions. The thermogram shows the T_g followed by m -cresol crystallization, followed by m -cresol remelting at the high m -cresol contents. As m -cresol content drops to 69.3 wt %, it no longer crystallizes and both the overshoot and magnitude of the T_g are greatly diminished. Concomitant increases in the liquid viscosity suggest greatly increased network formation, which is almost completed at 50% m -cresol. Inset: T_g vs m -cresol wt fraction. T_g of pure BPP is 44.2 $^\circ C$. (b) Indirect characterization of the T_g of Ti-BPA with cresol content <50%. These Ti-BPA samples have the same morphology before heating, as the overall cresol volume is small. After heating, the 40% cresol sample deformed and the 30% cresol sample clumped.

calorimetry but can only be qualitatively speculated by observing the morphology change of the MOF glasses upon heating. By heating the MOF glasses with different cresol composition at 200 °C overnight, the sample with no cresol retained its morphology, while the one with 30% cresol clumped and the one with 40% cresol deformed, indicating the glass can still flow even though no T_g can be observed. This is more like the classic behavior of alkali silicate glassformers, as the alkali oxide component is evaporated off, or of organic polymers, as cross-link density is maximized. The fact that the T_g disappears (Figure 4) while there is still so much *m*-cresol present strongly suggests that the network is already complete at 50% cresol, and the remaining solvent is sequestered in a dynamic plasticizing role in the intranetwork pore spaces (from which it is removed in the activation process).

This constructive approach to synthesizing MOF glasses is highly versatile, as multidentate alcohols and phenols can be used to substitute the BPA and BPP strut and still produce monolithic glasses. Flexible organic linkers, such as tetraethylene glycol, can also be incorporated in monolithic glasses (section S2, Figures S6 and S7). A functional molecule with hydroxyl groups can be mixed with BPA struts to produce functionalized MOF glasses, as exemplified by the incorporation of tetrakis(4-hydroxyphenyl)porphine (TPPP) molecule in the Ti-BPA glasses (Figure S8). In this experiment, 10% TPPP is mixed with BPA to give a purple glass with slightly higher porosity.

■ ASSOCIATED CONTENT

■ Supporting Information

The Supporting Information is available free of charge on the ACS Publications website at DOI: 10.1021/jacs.6b07078.

Details of synthesis and characterization (PDF)

■ AUTHOR INFORMATION

Corresponding Authors

*yaghi@berkeley.edu

*caa@asu.edu

Notes

The authors declare no competing financial interest.

■ ACKNOWLEDGMENTS

This work made use of facilities at the Molecular Foundry and Advanced Light Source BL 10.3.2. The Advanced Light Source and Molecular Foundry are supported by the Director, Office of Science, Office of Basic Energy Sciences, U.S. Department of Energy, under Contract No. DE-AC02-05CH11231. We acknowledge Mr. N. Kornienko for help on the MOF thin film preparation, Dr. Y. Ma and Prof. O. Terasaki for discussions on TEM, Dr. J. Guo and Dr. X. Feng for help and discussion of the EXAFS study, Dr. H. Furukawa for help on the density measurement, and Mr. J. Yang for help and discussion on nitrogen isotherm measurements. S.-Y.L. and C.A.A. acknowledge support of the U.S. Department of Energy under Contract No. DE-AC02-05CH11231, Subcontract No. 6920968, under the Batteries for Advanced Transportation Technologies Program. Partial financial support for aspects of the synthesis and porosity measurements is provided to O.M.Y. by BASF SE (Ludwigshafen, Germany) and King Abdulaziz City for Science and Technology (Riyadh, Saudi Arabia). Y.Z. acknowledges support of the Suzhou Industrial Park fellowship.

■ REFERENCES

- (1) (a) Zhou, H.-C.; Kitagawa, S. *Chem. Soc. Rev.* **2014**, *43*, 5415. (b) Furukawa, H.; Cordova, K. E.; O'Keeffe, M.; Yaghi, O. M. *Science* **2013**, *341*, 1230444. (c) Park, K. S.; Ni, Z.; Côté, A. P.; Choi, J. Y.; Huang, R.; Uribe-Romo, F. J.; Chae, H. K.; O'Keeffe, M.; Yaghi, O. M. *Proc. Natl. Acad. Sci. U. S. A.* **2006**, *103*, 10186. (d) Yaghi, O. M.; O'Keeffe, M.; Ockwig, N. W. E. A. *Nature* **2003**, *423*, 705.
- (2) (a) Phillips, J. C. *J. Non-Cryst. Solids* **1979**, *34*, 153. (b) Thorpe, M. F. *J. Non-Cryst. Solids* **1983**, *57*, 355. (c) He, H.; Thorpe, M. F. *Phys. Rev. Lett.* **1985**, *54*, 2107.
- (3) (a) Bennett, P. D.; Goodwin, A. L.; Dove, M. T.; Keen, D. A.; Tucker, M. G.; Barney, E. R.; Soper, A. K.; Bithell, E. G.; Tan, J.-C.; Cheetham, A. K. *Phys. Rev. Lett.* **2010**, *104*, 115503. (b) Chen, W.; Horike, S.; Umeyama, D.; Ogiwara, N.; Itakura, T.; Tassel, C.; Goto, Y.; Kageyama, H.; Kitagawa, S. *Angew. Chem., Int. Ed.* **2016**, *55*, 5195. (c) Bennett, T. D.; Tan, J.-C.; Yue, Y.-Z.; Baxter, E.; Ducati, C.; Terrill, N. J.; Cheetham, A. K.; Greaves, G. N. *Nat. Commun.* **2015**, *6*, 8079. (d) Bennett, T. D.; Yue, Y.; Li, P.; Qiao, A.; Tao, H.; Greaves, N. G.; Richards, T.; Lampronti, G. I.; Redfern, S. A. T.; Blanc, F.; Farha, O. K.; Hupp, J. T.; Cheetham, A. K.; Keen, D. A. *J. Am. Chem. Soc.* **2016**, *138*, 3484. (e) Umeyama, D.; Horike, S.; Inukai, M.; Itakura, T.; Kitagawa, S. *J. Am. Chem. Soc.* **2015**, *137*, 864.
- (4) Thornton, A. W.; Jelfs, K. E.; Konstantas, K.; Doherty, C. M.; Hill, A. J.; Cheetham, A. K.; Bennett, T. D. *Chem. Commun.* **2016**, *52*, 3750.
- (5) (a) Chapman, K. W.; Halder, G. J.; Chupas, P. J. *J. Am. Chem. Soc.* **2009**, *131*, 17546. (b) Bennett, T. D.; Cheetham, A. K. *Acc. Chem. Res.* **2014**, *47*, 1555.
- (6) McKeown, N. B.; Budd, P. M. *Chem. Soc. Rev.* **2006**, *35*, 675.
- (7) Schaate, A.; Roy, P.; Godt, A.; Lippke, J.; Waltz, F.; Wiebcke, M.; Behrens, P. *Chem. - Eur. J.* **2011**, *17*, 6643.
- (8) Suematsu, K.; Nakamura, K.; Takeda. *Colloid Polym. Sci.* **1983**, *261*, 493.
- (9) (a) Day, V. W.; Eberspacher, T. A.; Klemperer, W. G.; Park, C. W. *J. Am. Chem. Soc.* **1993**, *115*, 8469. (b) Fornasieri, G.; Rozes, L.; Le Calvé, S.; Alonso, B.; Massiot, D.; Rager, M. N.; Evain, M.; Boubekour, K.; Sanchez, C. *J. Am. Chem. Soc.* **2005**, *127*, 4869.
- (10) (a) Scolan, E.; Magnenet, C.; Massiot, D.; Sanchez, C. *J. Mater. Chem.* **1999**, *9*, 2467. (b) Soler-Illia, G. J. d. A. A.; Rozes, L.; Boggiano, M. K.; Sanchez, C.; Turrin, C.-O.; Caminade, A.-M.; Majoral, J.-P. *Angew. Chem., Int. Ed.* **2000**, *39*, 4249.
- (11) Adam, G.; Gibbs, J. H. *J. Chem. Phys.* **1965**, *43*, 139.
- (12) (a) Schmidt, H. *J. Non-Cryst. Solids* **1985**, *73*, 681. (b) MacKenzie, J. D.; Bescher, E. P. *J. Sol-Gel Sci. Technol.* **1998**, *13*, 371.
- (13) Farges, F.; Brown, G. E.; Rehr, J. J. *Phys. Rev. B: Condens. Matter Mater. Phys.* **1997**, *56*, 1809.
- (14) Vaid, T. P.; Tanski, J. M.; Pette, J. M.; Lobkovsky, E. B.; Wolczanski, P. T. *Inorg. Chem.* **1999**, *38*, 3394.
- (15) Greaves, G. N.; Meneau, F.; Sapelkin, A.; Colyer, L. M.; ap Gwynn, L.; Wade, S.; Sankar, G. *Nat. Mater.* **2003**, *2*, 622.
- (16) Elmer, T. H. *Engineered Materials Handbook*; ASM International, 1991; Vol. 4, p 427.
- (17) Cohen, M. H.; Turnbull, D. *Nature* **1964**, *203*, 964.
- (18) (a) Martinez, L. M.; Angell, C. A. *Nature* **2001**, *410*, 663. (b) Angell, C. A. *Science* **1995**, *267*, 1924.
- (19) Yue, Y.-Z. *Front. Mater.* **2014**, *2*, 054.
- (20) Amann-Winkel, K.; Gainaru, C.; Handle, P. H.; Seidl, M.; Nelson, H.; Böhmer, R.; Loerting, T. *Proc. Natl. Acad. Sci. U. S. A.* **2013**, *110*, 17720.
- (21) (a) Agladze, N. I.; Sievers, A. J. *Phys. Rev. Lett.* **1998**, *80*, 4209. (b) Liu, X.; Queen, D. R.; Metcalf, T. H.; Karel, J. E.; Hellman, F. *Phys. Rev. Lett.* **2014**, *113*, 025503.
- (22) Whalley, E.; Klug, D. D.; Handa, Y. P. *Nature* **1989**, *342*, 782.
- (23) (a) Greaves, G. N.; Sen, S. *Adv. Phys.* **2007**, *56*, 1. (b) Angell, C. A.; Moynihan, C. T.; Hemmati, M. *J. Non-Cryst. Solids* **2000**, *274*, 319.
- (24) Ellis, T. S.; Karasz, F. E.; Brinke, G. T. *J. Appl. Polym. Sci.* **1983**, *28*, 23.